Inorganic Chemistry

Article

pubs.acs.org/IC

Ferrocenyl-Functionalized Sn/Se and Sn/Te Complexes: Synthesis, Reactivity, Optical, and Electronic Properties

Zhiliang You,[†] Jakob Bergunde,[†] Birgit Gerke,[‡] Rainer Pöttgen,[‡] and Stefanie Dehnen*[,†]

[†]Fachbereich Chemie and Wissenschaftliches Zentrum für Materialwissenschaften, Philipps-Universität Marburg, Hans-Meerwein Strasse, D-35043 Marburg, Germany

[‡]Institut für Anorganische und Analytische Chemie, Universität Münster, Corrensstrasse 30, D-48149 Münster, Germany

Supporting Information

ABSTRACT: An adamantane-shaped, ferrocenyl-substituted tin selenide complex, $[(FcSn)_4Se_6]$ (**1**; Fc = ferrocenyl), and a ferrocenyl-substituted tin telluride five-membered ring, $[(Fc_2Sn)_3Te_2]$ (**2**), were obtained upon treatment of $FcSnCl_3$ with K_2E (E = Se, Te). Complex **1** further reacts with $Na_2S\cdot 9H_2O$ and $[Cu(PPh_3)_3Cl]$ to form a ternary complex, $[(CuPPh_3)_6(S/Se)_6(SnFc)_2]$ (**3**). We discuss structures, optical and electrochemical properties as well as Mössbauer spectra.

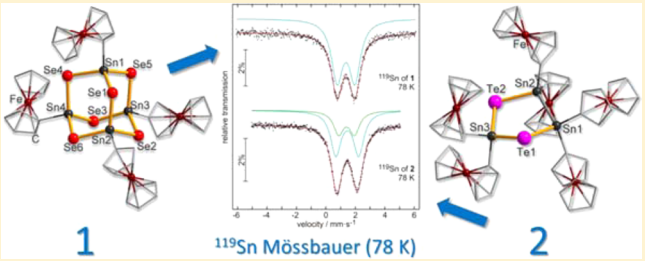

INTRODUCTION

Metalchalcogenides and chalcogenidometalates belong to the most actively investigated inorganic materials. Because of the progress in modern preparative and structural methods, a huge variety of molecular, nanostructured, or mesostructured derivatives with different compositions and diverse structures have been synthesized, showing a broad range of chemical and physical properties.[1] For instance, inorganic chalcogenide cluster-based open frameworks that were synthesized in solvothermal reactions exhibit diverse topologies, which combine high porosity, high surface area, and electrical and ionic conductivity with tunable optoelectronic properties.[2] Molecular species, such as the extensively studied CdE clusters (E = S, Se, and/or Te) are known for showing size-dependent optical and electronic properties.[3] Fine-tuning of optoelectronic and also magnetic properties was furthermore achieved by combination of different transition and/or main-group elements in such systems.[4]

Besides some polymeric structures,[5] organo-decorated metal chalcogenides, especially those of main-group metal chalcogenides, are essentially restricted to the molecular level. Recent developments in this field include new synthetic approaches, reactivity, and further extension of both the inorganic and the organic part of such complexes.[6,7] For this, chalcogenidotetrelate complexes of the general composition $[(RT)_xE_y]$ (R = organic ligand; T = Sn, Ge; E = S, Se, Te), which are based on an adamantane-type (AD) or double-decker-type (DD) inorganic core, that have been known for a long time with nonreactive ligands like Me, Ph, ^{t}Bu, CF_3, C_6F_5, $C(SiMe_3)_3$,[8] were recently decorated with functional organic ligands R^f, such as R^1(H) = C_2H_4COO(H) or R^2 = $CMe_2CH_2C(Me)O$, the latter of which is reactive toward hydrazine, organylhydrazines, hydrazones, or hydrazides.[6a,d,7]

Some examples of Sn/S cages have additionally been reported that were surrounded by mono- (Fc) or bis-functionalized (fC) ferrocenyl units.[9,10] This way, it was possible to study the influence of this specific organometallic ligand on the structural and electrochemical properties of the core.

First investigations were undertaken through the attachment of mono- and bis-substituted ferrocenyl ligands to organo-functionalized precursor DD-type complexes. The resulting Fc-terminated Sn/S complexes, which underwent rearrangement into a larger $[Sn_6S_{10}]$ skeleton during the functionalization reaction, showed intramolecular electronic communication between the different Fc units due to their dynamics in solution.[9] In the case of bis-functionalized ferrocene ligands, the DD inorganic core was retained during ligand attachment, and the more rigid complexes exhibited different electrochemical stabilities as dependent from the mode of linkage between the Sn/S core and the fC unit.[10,11]

An alternative strategy is to directly attach Fc units to the inorganic core. Two different approaches have been reported until now. By treatment of $CdCl_2$ with silylated selenoferrocene (TMSSeFc, TMS = $-SiMe_3$), the Fc-functionalized AD-type Cd/Se complex was synthesized; cyclic voltammetry (CV) measurements, however, indicated instability of the inorganic core during electrochemical treatment.[12] The direct substitution of Sn atoms has been realized in our group by treatment of $FcSnCl_3$ (**A**) with Na_2S in tetrahydrofuran (THF). The resulting AD-type Sn/S complex $[(FcSn)_4S_6]$ (**B**) was investigated by means of ^{119}Sn Mössbauer spectroscopy, which showed a weak electrochemical interplay.[13]

Received: August 21, 2014
Published: November 14, 2014

   dx.doi.org/10.1021/ic502026g | Inorg. Chem. 2014, 53, 12512−12518

Our current work intended to extend the investigations of Fc-functionalized Sn/S complexes by treatment of **A** with the heavier chalcogenides E = Se, Te to generate Fc-functionalized Sn/E complexes. As our first results, we report herein the synthesis of $[(FcSn)_4Se_6]$ (**1**), the heavier homologue of **B**, and $[(Fc_2Sn)_3Te_2]$ (**2**), along with their structures and optical and electrochemical properties. Furthermore, **1** was subject to further extension of the inorganic core to form the multinary, Fc-functionalized cluster $[(CuPPh_3)_6(S/Se)_6(SnFc)_2]$ (**3**).

EXPERIMENTAL SECTION

Syntheses. *General.* All reaction steps were carried out under Ar atmosphere, unless otherwise noted. All solvents were dried and freshly distilled prior to use. Ferrocenyltintrichloride ($FcSnCl_3$), potassium selenide (K_2Se), potassium telluride (K_2Te), and $[Cu(PPh_3)_3Cl]$ were prepared according to the reported methods.[13−15] CuCl and PPh_3 were purchased from Sigma-Aldrich.

*Synthesis and Analysis of $FcSnCl_3$ (**A**).* The precursor $FcSnCl_3$ was prepared according to the reported method.[13] Here, the NMR analyses of $FcSnCl_3$ were carried in deuterated chloroform ($CDCl_3$) instead of deuterated benzene to understand the change of electronic situation on Fc-substituted Sn atoms in comparison with resulting products, because of the influence of solvent effect on the chemical shifts, especially for the ^{119}Sn NMR. ^{1}H NMR: (300 MHz, $CDCl_3$): δ = 4.66, 4.42 (2 × m, 2 × 2H, $Cp_{subst.}$-*H*), 4.37 (s, 5H, $Cp_{unsubst.}$-*H*) ppm; ^{13}C NMR: (75 MHz, $CDCl_3$): δ = 73.1, 72.6, 72.5 ($Cp_{subst.}$-*C*), 70.3 ($Cp_{unsubst.}$-*C*) ppm; ^{119}Sn NMR: (186 MHz, $CDCl_3$): δ = −14.8 ppm.

*Synthesis of $[(FcSn)_4S_6]$ (**B**).* The synthesis of tin sulfide AD-type complex **B** was slightly modified according to the reported synthetic pathway.[13] $FcSnCl_3$ (0.212 g, 0.52 mmol) and Na_2S (0.601 g, 0.77 mmol) were suspended in 18 mL of THF. After 1 d of stirring at room temperature (rt), the solvent was evaporated in vacuum, and the residues were extracted with 10 mL of $CHCl_3$. The yellow extract was layered with *n*-pentane (1:1) and stored in a freezer. Yellow needle-shaped crystals of **B** were obtained within a week. Yield: 0.127 g, 74% (calculated on the basis of $FcSnCl_3$). ^{1}H NMR: (300 MHz, $CDCl_3$): δ = 4.53, 4.42 (2 × m, 2 × 8H, $Cp_{subst.}$-*H*), 4.38 (s, 20H, $Cp_{unsubst.}$-*H*) ppm; ^{13}C NMR: (75 MHz, $CDCl_3$): δ = 75.1, 72.8, 71.6 ($Cp_{subst.}$-*C*), 69.8 ($Cp_{unsubst.}$-*C*) ppm; ^{119}Sn NMR: (186 MHz, $CDCl_3$): δ = 112.1 ppm.

*Synthesis of $[(FcSn)_4Se_6]$ (**1**).* $FcSnCl_3$ (0.201 g, 0.49 mmol) and K_2Se (0.120 g, 0.76 mmol) were suspended in 18 mL of THF. After 2 d of stirring at rt, the solvent was evaporated in vacuum, and the residues were extracted with 10 mL of $CHCl_3$. The red extract was layered with *n*-pentane (1:1) and stored in a freezer. Orange plate-shaped crystals of **1** were obtained within a week. Yield: 0.156 g, 76% (calculated on the basis of $FcSnCl_3$). ^{1}H NMR: (300 MHz, $CDCl_3$): δ = 4.52, 4.43 (2 × m, 2 × 8H, $Cp_{subst.}$-*H*), 4.38 (s, 20H, $Cp_{unsubst.}$-*H*) ppm; ^{13}C NMR: (75 MHz, $CDCl_3$): δ = 74.5, 72.7, 71.3 ($Cp_{subst.}$-*C*), 69.8 ($Cp_{unsubst.}$-*C*) ppm; ^{119}Sn NMR: (186 MHz, $CDCl_3$): δ = −85.8 ppm, $^1J(^{119}Sn^{77}Se)$ = 1470 Hz; ^{77}Se NMR: (95 MHz, $CDCl_3$): δ = −111.0 ppm; ESI-MS(+): *m*/*z* = 1712.1 ($[M + Na]^+$); 1689.1 ($[M]^+$); IR: $\tilde{\upsilon}/cm^{-1}$ = 3087 (m), 2395 (s), 2340 (s), 2282 (s), 2071 (w), 2043 (w), 2009 (w), 1976 (w), 1780 (w), 1635 (w), 1407 (m), 1376 (m), 1301 (m), 1187 (m), 1138 (s), 1104 (m), 1050 (s), 4018 (s), 996 (s), 898 (m), 871 (m), 819 (s), 757 (m), 732 (m), 630 (m), 593 (m), 481 (s).

*Synthesis of $[(Fc_2Sn)_3Te_2]$ (**2**).* $FcSnCl_3$ (0.153 g, 0.37 mmol) and K_2Te (0.116 g, 0.56 mmol) were suspended in 18 mL of THF. After 2 d of stirring at rt, the solvent was evaporated in vacuum, and the residues were extracted with 8 mL of dichloromethane. The orange-yellow extract was layered with *n*-pentane (1:1), and stored in a freezer. Orange-red block-shape crystals of **2** were obtained within a week. Yield: 0.050 g, 24% (calculated on the basis of $FcSnCl_3$). ^{1}H NMR: (500 MHz, $CDCl_3$): δ = 4.47−4.42 (4 × m, 4 × 4H, $Cp_{subst.}$-*H* in four Fc units connected with a Sn−Sn dumbbell), 4.34, 4.32 (2 × m, 2 × 4H, $Cp_{subst.}$-*H* in two Fc units connected with a Sn(IV) atom), 4.28 (s, 10H, $Cp_{unsubst.}$-*H* in two Fc units connected with a Sn(IV) atom), 4.16 (s, 20H, $Cp_{unsubst.}$-*H* in four Fc units connected with a Sn−Sn dumbbell) ppm; ^{13}C NMR: (125 MHz, $CDCl_3$): δ = 75.1, 75.0, 71.8 ($Cp_{subst.}$-*C* in two Fc units connected to a Sn(IV) atom), 74.4, 71.2, 71.2, 71.0, 70.9, 69.0 ($Cp_{subst.}$-*C* in four Fc units connected to a Sn−Sn dumbbell), 69.4 ($Cp_{unsubst.}$-*C* in two Fc units connected with a Sn(IV) atom), 69.3 ($Cp_{unsubst.}$-*C* in four Fc units connected with a Sn−Sn dumbbell) ppm; ^{119}Sn NMR: (186 MHz, $CDCl_3$): δ = −36.9, −196.9 ppm; ^{125}Te NMR: (158 MHz, $CDCl_3$): δ = −1038.9 ppm; ESI-MS(+): *m*/*z* = 1744.5 ($[M + Na]^+$); IR: $\tilde{\upsilon}/cm^{-1}$ = 3915 (w, br), 3084 (m, br), 2350 (w), 2050 (w), 1636 (w), 1406 (m), 1373 (m), 1297 (m), 1260 (w), 1181 (m), 1134 (s), 1104 (s), 1049 (m), 1019 (s), 998 (s), 870 (m), 817(vs), 737 (m), 603 (m), 496 (vs), 478 (vs), 405 (m).

*Synthesis of $[(CuPPh_3)_6(S/Se)_6(SnFc)_2]$ (**3**).* To compound **1** (0.0397 g, 0.0235 mmol) and $Na_2S{\cdot}9H_2O$ (0.0349 g, 0.141 mmol), the solvents THF (5 mL) and water (1 mL) were added one after the other. After 15 min of stirring, the generated clear yellow solution was added to the mixture of $[CuCl(PPh_3)_3]$ (0.250 g, 0.282 mmol) in 5 mL of THF. The solution turned to red-brown. It was stirred for 12 h and then filtered. The solution was layered over water (1:1). Light yellow crystals of **3** were obtained within 2 d. Yield: 0.024 g, 33% (calculated on the basis of **1**). ^{1}H NMR: (500 MHz, CD_2Cl_2): δ = 7.75−7.66, 7.60−7.45 (m, 90H, *H*-Ar), 3.74, 1.85 (m, 16H, *H*-THF) ppm. ^{31}P NMR: (202 MHz, CD_2Cl_2): δ = 43.9, 35.9 ppm. ^{119}Sn NMR: (186 MHz, CD_2Cl_2): δ = 153.9, −71.8 ppm. IR: $\tilde{\upsilon}/cm^{-1}$ = 2963 (w), 2341, 2361 (w, br), 1432 (w), 1477 (w), 1408 (w), 1259 (m), 1084 (br, m), 1013 (s), 868 (w), 792 (s), 743 (m), 689 (m), 563 (w), 482 (m).

NMR Spectroscopy. ^{1}H, ^{13}C, ^{119}Sn, ^{77}Se, and ^{125}Te NMR measurements were carried out using a Bruker DRX 300 or 500 MHz spectrometer at 25 °C. In ^{1}H and ^{13}C NMR spectra, the chemical shifts were quoted in ppm relative to the residual protons of deuterated solvents. In ^{119}Sn, ^{77}Se, and ^{125}Te NMR analyses, Me_4Sn, $(CH_3)_2Se$, and $(CH_3)_2Te$ were used as internal standard, respectively.

Infrared Spectroscopy. Infrared (IR) spectra were recorded on a Bruker TENSOR 37 FT-IR spectrometer.

Raman Spectroscopy. Raman spectra were recorded on a Labram HR 800 Raman spectrometer with a 632.8 nm red laser in the range of 80−3200 cm^{-1}. The beam was focused on the sample through a confocal microscope using a 50× objective lens.

UV−Visible Absorption Spectroscopy. UV−visible absorption spectra were recorded on a PerkinElmer Cary 5000 UV/vis/NIR spectrometer in the range of 800−200 nm, employing the double-beam technique. The samples were prepared as solution in CH_2Cl_2.

Energy-Dispersive X-ray (EDX) Spectroscopy. EDX analyses were performed using the EDX device Voyager 4.0 of Noran Instruments coupled with the electron microscope CamScan CS 4DV. Data acquisition was performed with an acceleration voltage of 20 kV and 100 s accumulation time. For the analyses, multiple single crystals were used, and the data recorded both various times on one single crystal and various times on other single crystals.

Electrospray Ionization (ESI) Mass spectrometry. ESI-MS was performed on a Finnigan MAT 95S. The electrospray ionization ion trap mass spectrometry (ESI-ITMS) spectra were obtained by using solvent as the carrier gas.

^{57}Fe and ^{119}Sn Mössbauer Spectroscopy. $Ca^{119m}SnO_3$ and ^{57}Co/Rh sources were used for the Mössbauer spectroscopic experiments. The measurements were carried out at 78 and 5 K in transmission geometry. The Mössbauer sources were kept at room temperature. Polycrystalline samples of **1** and **2** were diluted with dry SiO_2 and enclosed in small PMMA containers. For the ^{119}Sn measurements a palladium foil of 0.05 mm thickness was used to reduce tin K X-rays concurrently emitted by this source. Fitting of the spectrum was performed with the Normos-90 program system.[16]

Electrochemical Measurements. All electrochemical measurements—cyclic and differential pulse voltammetry (CV and DPV)—were recorded under Ar atmosphere at 25 °C, using 0.1 mol/L $[^nBu_4N][PF_6]$ as the supporting electrolyte. The potentials were referenced internally to ferrocene, added at the end of the experiments.

dx.doi.org/10.1021/ic502026g | Inorg. Chem. 2014, 53, 12512−12518

Table 1. Crystallographic and Refinement Details of 1−3

compound	1	2	3
chemical formula	$C_{40}H_{36}Fe_4Se_6Sn_4$	$C_{60}H_{54}Fe_6Sn_3Te_2$	$C_{136}H_{120}Fe_2Se_{3.25}S_{2.75}Sn_2Cu_6P_6O_4$
formula mass/g·mol^{-1}	1688.61	1721.40	3079.24
crystal color and shape	orange plate	orange-red block	yellow block
crystal size/mm^3	0.22 × 0.15 × 0.08	0.26 × 0.14 × 0.03	0.16 × 0.16 × 0.14
crystal system	orthorhombic	triclinic	monoclinic
a/Å	24.9134(6)	12.5690(4)	42.3467(11)
b/Å	13.2096(4)	12.8600(4)	14.5072(4)
c/Å	27.1065(8)	17.9930(6)	42.7189(11)
α/deg	90	105.6830(10)	90
β/deg	90	95.6560(10)	92.544(1)
γ/deg	90	102.2110(10)	90
V/Å^3	8920.6(4)	2698.98(15)	26217.7(12)
space group	*Pbca*	$P\bar{1}$	*C*2/*c*
Z	8	2	8
radiation type	Mo Kα	Mo Kα	Mo Kα
abs. coefficient, μ/mm^{-1}	8.4	4.0	2.6
abs. correction type	multiscan	multiscan	multiscan
max/min transmission	0.553/0.260	0.889/0.421	0.685/0.663
2θ range/deg	4.4−54.3	4.4−50.0	4.8−50.0
no. of reflections meas.	60 834	45 121	173 710
no. of ind. reflections	9863	9483	22998
R_{int}	0.0923	0.0293	0.074
R_1 ($I > 2\sigma(I)$)/$wR(F^2)$ (all data)	0.0338/0.0841	0.0237/0.0608	0.063/0.189
goodness of fit on F^2	1.041	1.042	1.08
largest diff. peak/hole, e$^-$·Å^{-3}	0.87/−0.95	3.49/−0.78	1.94/−1.20

Scheme 1. Synthesis of Compounds 1 and 2 by Reactions of $FcSnCl_3$ with K_2E (E = Se, Te). By Further Treatment of 1 with $Na_2S·9H_2O$ and Ensuing Reaction with $[Cu(PPh_3)_3Cl]$, the Cluster Compound 3 was Obtained

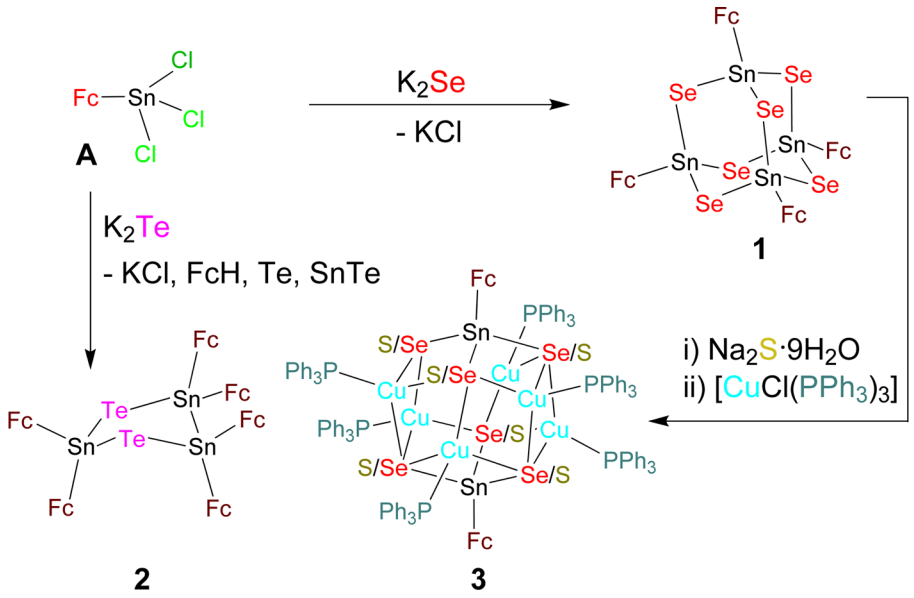

Working and counter electrodes: Pt; scan rate: 200 mV/s; pulse amplitude for DPV: 50 mV.

X-ray Diffraction Measurement, Structure Solution, and Refinement. Data were collected on a diffractometer equipped with a Bruker PHOTON 100 detector system D8 QUEST, using graphite-monochromatized Mo Kα radiation (λ = 0.710 73 Å) at 100 K. The structure solution and refinement were performed by Sir-2004,[17] and full-matrix-least-squares refinement against F^2 was done using the SHELXL-2013 software.[18] Details of the data collections and refinements are given in Table 1. Selected structural parameters are provided in Supporting Information, Tables S6−S10, S12, and S13. S versus Se atomic disorder in compound **3** was modeled by using the PART instruction with EADP during the refinement, ending up with independent positions of both atoms (see Supporting Information, Figure S18 and Table S11). The resulting S/Se ratio (2.71:3.29) is very close to that determined via EDX spectroscopy (2.71:3.25, see Supporting Information, Table S5).

RESULTS AND DISCUSSION

Treatment of **A** with 1.5 equiv of K_2Se in THF yielded a Fc-substituted AD-type Sn/Se complex, $[(FcSn)_4Se_6]$ (**1**), along

dx.doi.org/10.1021/ic502026g | Inorg. Chem. 2014, 53, 12512−12518

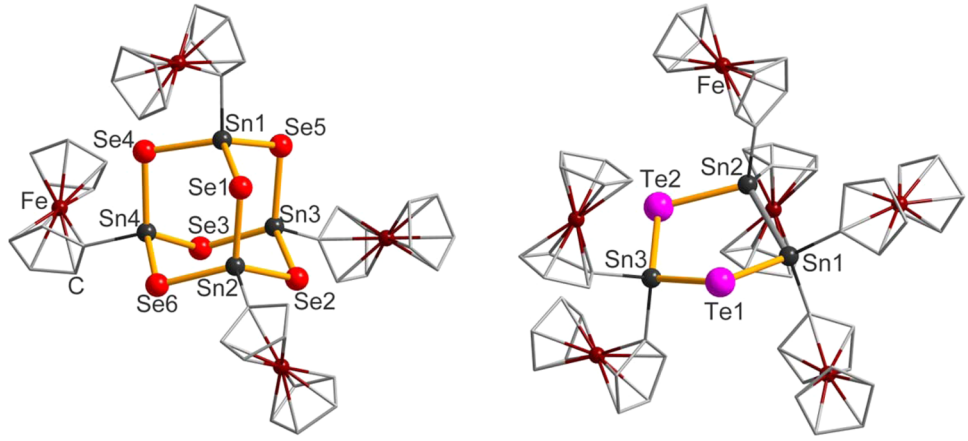

Figure 1. Molecular structures of **1** (left) and **2** (right), without H atoms.

with KCl in a clean reaction. A similar reaction with 1.5 equiv of K_2Te under the same conditions, however, led to the formation of a puckered five-membered Sn/Te ring with bis-substituted Sn atoms, $[(Fc_2Sn)_3Te_2]$ (**2**), besides KCl and a black residue containing Fe, Sn, and Te according to energy dispersive X-ray (EDX) spectroscopy (Supporting Information, Figure S9, Table S4). Owing to a slight excess of Te, we suppose that it comprises a mixture of ferrocene, SnTe, and Te, which is in agreement with an earlier report.[19] Treatment of **1** with 6 equiv of $Na_2S{\cdot}9H_2O$ to initially break up Sn−E bonds, and subsequent reaction of the mixture with 12 equiv of $[CuCl(PPh_3)_3]$ in THF/H_2O, led to the formation of the cluster $[(CuPPh_3)_6(S/Se)_6(SnFc)_2]$ (**3**; Scheme 1). All compounds are air stable in the solid state, well-soluble in chlorinated solvents, and were characterized by standard analytic techniques (see Supporting Information). The molecular structures were determined by single-crystal X-ray diffraction (XRD; see the Experimental Section).

The nearly tetrahedral, AD-type $[Sn_4Se_6]$ core in **1** is decorated by Sn−C-bound Fc units (Figure 1 left), as observed for its sulfide analog **B**. All Sn atoms have the same coordination sphere; they are surrounded by three Se atoms and one Fc unit. Sn−Se bond lengths (2.5130(7)−2.5457(7) Å) and Sn−C bond lengths (2.096(5) and 2.111(5) Å) are in agreement with those reported for the related compound $[(PhSe)_3Sn{-}fC{-}Sn(SePh)_3]$ (2.5058(11)−2.5413(11) Å for Sn−Se; 2.1040(7) Å for Sn−C).[20]

Unexpectedly, the reaction of **A** with the K_2Te did not afford the ubiquitous AD-type cluster topology but the five-membered ring-based Sn/Te complex **2** (Figure 1 right). The ring contains one isolated Sn atom and a Sn−Sn bond, and therefore two types of Sn atoms. This is clearly reflected by two ^{119}Sn NMR signals (−36.9 and −196.9 ppm) with relative intensities close to 2:1 (Supporting Information, Figure S3). Sn1 and Sn2, which are involved in the Sn−Sn bond, are additionally coordinated by two Fc units and one Te atom. Sn3 is bonded to two Fc units and two Te atoms. All Sn atoms therefore adopt nearly tetrahedral coordination geometry. The same inorganic structural motif, however, exhibiting different organic decorations and not only Te, but also S or Se within the ring, $[(R_2Sn)_3E_2]$ (R = ^{t}Bu, Me; E = S, Se, Te), has been independently reported by Puff and Mathiasch.[19,21] Unlike **2**, these compounds were synthesized either by oxidation of cyclic organostannanes (Sn^{II}) or organotin hydrides with elemental chalcogens or through reduction of organotin chalcogenide four-membered rings (Sn^{IV}) with lithium aluminum hydride.[19,21d,22] We assume that the reductive nature of Te^{2-} ($E^\circ_{1/2}$ = −1.143 V)[23] causes Sn−Sn bond formation under production of elemental Te. Ge−Ge bond formation within a telluridogermanate complex was recently observed under similar conditions.[6c] To rationalize the change from a monosubstituted Sn atom in **A** to all bisubstituted Sn atoms, it should be mentioned that the C−Sn bond is known to be labile for C being part of an aryl or a straight-chain alkyl group in the presence of Lewis acids. A prominent example for this is the Kocheshkov redistribution reaction of SnX_4 with $R'SnR_3$ to form $R'SnCl_3$,[24] which allows to explain the findings as a redistribution of Fc units occurring along with the redox reaction. The Sn−Sn bond in **2** (2.7952(3) Å) is slightly shorter than that observed in the related compound $[(^tBu_2Sn)_3Te_2]$ (2.836(2) or 2.843(2) Å),[21d] which might be attributed to the even bulkier ^{t}Bu ligands. The less-affected Sn−Te distances are therefore very similar, ranging from 2.7266(3) to 2.7558(3) Å in both compounds.

The optoelectronic properties of **1** and **2**, and the previously unexplored properties of **B**, were examined by UV−visible absorption spectroscopy in CH_2Cl_2 solutions (Supporting Information, Figure S4). In all three compounds, the absorption bands of the ferrocenyl group were red-shifted with respect to the absorption of pure ferrocene—more significantly as the chalcogenide changed from S through Se to Te. According to the color changes observed for purely inorganic Sn/E complexes,[4a−d] the named variation of the chalcogenide ligands also caused a red shift of the p(E) → s,p(Sn) charge transfer band, even though the structures of the three complexes are not exactly the same and even differ by the number of Sn or E atoms.

To study the impact of both structural changes as well as replacement of one chalcogen by another on the electrochemical properties, cyclic and differential pulse voltammetry (CV and DPV) were run on CH_2Cl_2 solutions of **1**, **2**, and **B**. The voltammograms of **B** and **1** are shown in Figure 2.

Both compounds undergo a single-step oxidation Fe^{2+} → Fe^{3+} in the CV mode (E_{pa} = 450 mV for **B**, 370 mV for **1**), indicating four eqivalent and widely independent redox sites in each compound. The DPV measurements confirm this finding in that only one oxidation peak is observed for each compound; however, the peaks are relatively broad, which is indicative of some communications of the redox sites due to movement of the Fc units in solution. In the case of the sulfide complex **B**, a

dx.doi.org/10.1021/ic502026g | Inorg. Chem. 2014, 53, 12512−12518

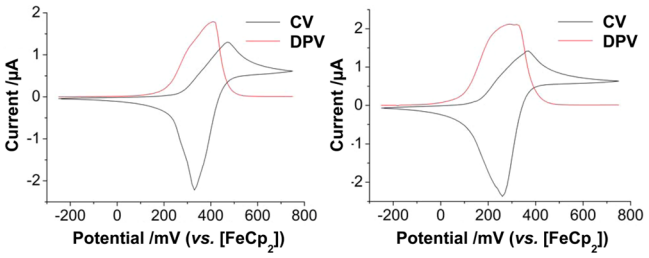

Figure 2. Cyclic and differential pulse voltammograms, recorded at a platinum electrode in CH_2Cl_2 solutions of the sulfide complex **B** (1.60 mM, left) or the selenide complex **1** (1.53 mM, right) in the presence of tetra-*n*-butylammonium hexanfluorophosphate (TBFP) (0.1 M). Scan ranges and rates: CV, −220 to 800 mV, 200 mV/s; DPV, −220 to 800 mV, 10 mV/s. Pulse amplitude 50 mV.

trend toward separation of the peaks is visible, whereas in the case of the selenide complex **1**, both measurements show that the chalcogenide ligand influences the redox properties of the Fc unit, in that the redox potential decreases upon replacing E = S with E = Se, in accordance with a decreased electron withdrawal from the adjacent Sn atoms and consequently slight increase of the electron density within the Cp rings, in turn enabling easier oxidation of the Fe ions. The fact that the cathodic return wave is higher and thinner than the anodic forward wave in both compounds is assumed to be due to an interaction of the Sn/E skeleton with the electrodes in the present case. Different as for nanoparticles bearing ferrocenenyl termini[25] and ferrocene-based Ag/Se clusters,[26] where the effect was reported to be attributed to an adsorption of the ferrocenium form of the complexes onto the electrode, the title compounds here are not terminated by a functional group that would influence the wave shape in CV.[25] The assumption for a contribution of the Sn/E skeleton agrees with the overall tendency of chalcogenides to interact with metal surfaces.[27] Whereas bulkier organic ligands seem to effectively protect the Sn/E complexes from an attachment to the electrode material,[10] the ferrocenyl groups in **1** and **B** do not seem to form a sufficiently protective shield (Supporting Information, Figures S16, S17). Still, the adsorption does not seem to proceed further toward any decomposition of the compounds, as the CV redox waves remained the same after several scans without any intensity drop. The difference between the anodic and cathodic peak potentials (ΔE_p) is slightly shifted from 140 mV in **B** to 110 mV in **1** (Supporting Information, Table S1), suggesting a somewhat stronger interaction of the selenide cluster with the electrode surface as compared to the sulfide cluster.

At first glance, the CV voltammogram of **2** is similar to those of **B** and **1** in that it also exhibits an almost single-step oxidation. However, the oxidation range is even broader and combined with a large and thin cathodic return wave. Additionally, the DPV measurement shows much more complicated oxidation processes going on at the six Fc units in **2**. As indicated by two broad shoulders occurring along the oxidation peak, interactions between the iron centers are very probable here due to the shorter intramolecular Fe···Fe distances (8.30−10.59 Å in **1** and 8.11−9.98 Å in **B** vs 5.53−10.46 Å in **2**; see also Supporting Information, Tables S8−10). Both interactions through the bridging Sn atom of terminal Fc groups and/or through space are thus possible here.

As local probe for the electronic situation of the tin atoms in the cluster core and the iron atoms in the ferrocenyl groups ^{119}Sn and ^{57}Fe Mössbauer spectroscopic measurements were carried out on compounds **1** and **2**. The results are summarized in Figure 3 and Table 2.

Table 2. Fitting Parameters of ^{57}Fe and ^{119}Sn Mössbauer Spectroscopic Measurements of Compounds 1 and 2

T/K	source	δ^a/mm·s^{-1}	$\Delta E_Q{}^b$/mm·s^{-1}	Γ^c/mm·s^{-1}	ratio/%
1					
78	^{119}Sn	1.36(1)	1.21(1)	0.93(1)	100
5	^{57}Fe	0.43(1)	2.39(1)	0.29(1)	100
2					
78	^{119}Sn	1.40(1)	1.08(2)	0.82(3)	33[d]
		1.45(1)	1.55(1)	0.86(1)	67[d]
5	^{57}Fe	0.44(1)	2.39(1)	0.56(1)	100

[a]δ = isomer shift. [b]ΔE_Q = electric quadrupole splitting. [c]Γ = experimental line width. [d]This parameter was kept fixed during the fitting procedure.

The ^{57}Fe and ^{119}Sn spectra of **1** show a great accordance with the spectra of the S analogue **B**. The ^{119}Sn isomer shift of 1.36(1) mm·s^{-1} is slightly increased compared to 1.28(1) mm·s^{-1} of **B** due to a slight decrease in electronegativity when going

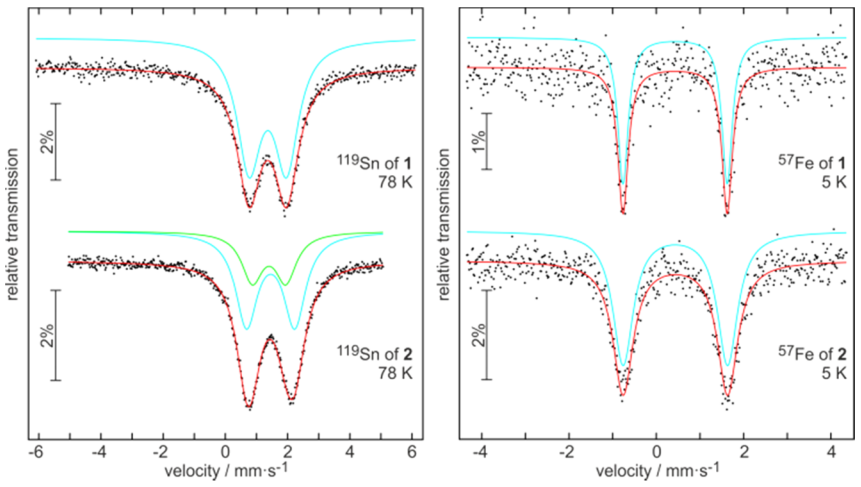

Figure 3. ^{119}Sn (left) and ^{57}Fe (right) Mössbauer spectra of **1** (upper) and **2** (lower).

dx.doi.org/10.1021/ic502026g | Inorg. Chem. 2014, 53, 12512−12518

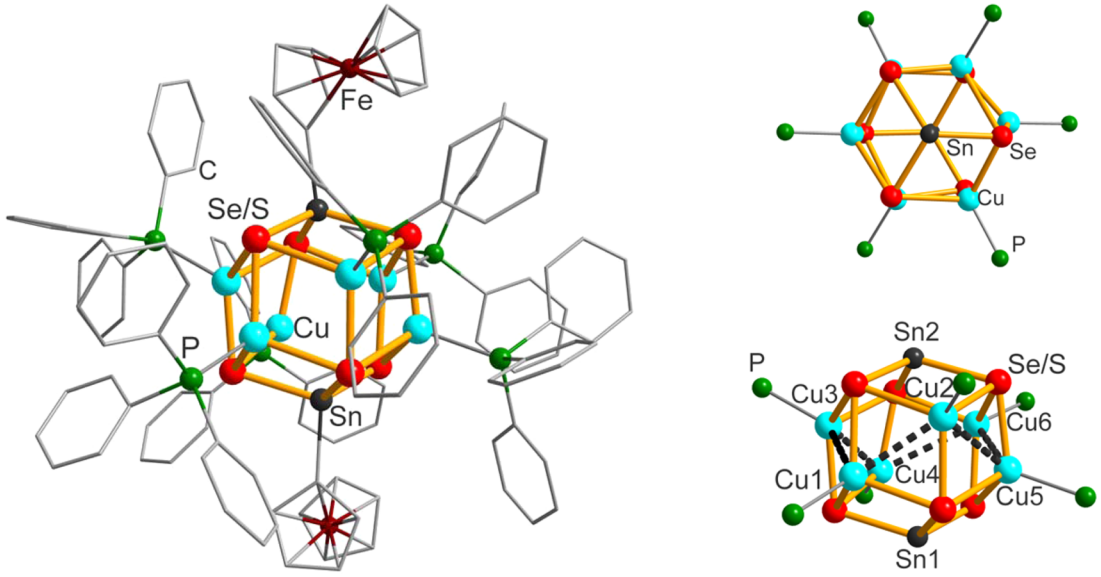

Figure 4. Different views of the molecular structure of **3**, without H atoms (left), further without Fc units and phenyl rings (right), viewed in two different orientations (top and bottom). The chair conformation of six Cu atoms is highlighted by dashed black lines (lower right).

from sulfur to selenium, which results in a higher s-electron density at the tin nucleus. The quadrupole splitting resulting from the noncubic site symmetry of the tin atoms is 1.21(1) $mm \cdot s^{-1}$ and therefore almost identical with the refined splitting of **B**. The ^{57}Fe spectrum was well-reproduced with a single signal, subjected to quadrupole splitting. The single signals of the four crystallographically independent tin atoms superimpose, indicating almost similar electronic situation.

The two tin sites in **2** can be distinguished in the ^{119}Sn spectrum, with those of the Sn−Sn dumbbell showing slightly higher isomer shifts (i.e., slightly higher s-electron density) and enhanced quadrupole splitting (a consequence of the higher site asymmetry). The symmetry of the Sn_3Te_2 core is much lower than that of the adamantane-related Sn_4Se_6 core, leading to larger differences for the six independent ferrocenyl groups. Again, we could reproduce the ^{57}Fe spectrum with a single signal, however, with an enhanced line width accounting for the superposition of six single signals.

Combination of organic binary chalcogenidostannate anions $[SnE^1_4]^{4-}$ with chalcogenides like K_2E^2 ($E^1 \neq E^2$) in protic solvents comes along with an exchange of chalcogenide ligands and the formation of mixed chalcogenidometalate anions $[SnE^1_{4-x}E^2_x]^{4-4f}$ or $[M_4Sn_4E^1_{17-x}E^2_x]^{10-}$.[4f,g] However, ternary organotin−metalchalcogenide complexes with different chalcogenides have not been reported so far. To check the availability of the latter, we treated the organotin selenide compound **1** with $Na_2S \cdot 9H_2O$ first and subsequently with $[CuCl(PPh_3)_3]$ in THF/H_2O, which indeed yielded the mixed-chalcogenide cluster compound **3** (Figure 4), which is isostructural with the known complexes $[(PhSn)_2(CuPMe_2Ph)_6S_6]$ (**C**)[8a] and $[(R^{1,2}T)_2(CuPPh_3)_6S_6]$ (T = Sn, **D**; T = Ge, **E**).[6a] Compound **3** comprises a polynuclear inorganic Cu/Sn/E core, which is shielded by PPh_3 ligands and Fc units attached to the Cu and Sn atoms, respectively.

The $Cu_6Sn_2(S,Se)_6$ architecture represents a rhombic dodecahedron, formed by 2-fold capping of a (nonbonded) chair arrangement of six Cu atoms through two E_3SnFc units. The latter were formed by nucleophilic attack of the AD-type Sn/Se complex in **1** by 6 equiv of S^{2-} anions in aqueous THF solution. According to previously reported NMR studies on chalcogenide exchange reactions, which led to the formation of purely inorganic $[SnSe_xS_{4-x}]^{4-}$ or $[SnSe_xS_{3-x}]^{2-}$ anions,[4g] the two ^{119}Sn MNR signals that were observed for a solution of **3** (δ = 153.9, −71.8 ppm, $\Delta\delta$ = 126 ppm; see Experimental Section) indicate that the initial treatment of **1** has most probably produced two $[FcSnSSe_2]^{3-}$ and two $[FcSnS_2Se]^{3-}$ anions per formula unit of the reactant; this is supported by a spectrum of a fresh mixture of **1** with 6 equiv of $Na_2S \cdot 9H_2O$ in a 5:1 THF/D_2O mixture at room temperature (as for the synthesis of **3** before addition of the copper complex), which shows two new signals beside that of **1** in a 1:1 ratio (see Supporting Information, Figure S20). Because of mixed occupancy of the chalcogenide positions by S and Se atoms in **3**, their distribution within the molecule could not be rationalized by the crystal structure analysis; however, the assumption is in agreement with the overall S/Se ratio gathered from the crystal structure refinement and observed by means of EDX analyses (Supporting Information, Figure S10; Tables S5, S11), both of which point toward a near 1:1 situation (S/Se = 1:1.2). Disregarding a slight excess of Se atoms, the ratio of heavy atoms in **3** is thus exactly the same as in the reaction mixture. The partial substitution of S with Se atoms clearly influences the bond lengths (Sn−E, 2.4521(12)−2.4919(10) Å; Cu−E, 2.3336(13)−2.8304(15) Å), which are significantly longer than those in the Sn/S or Ge/S compounds **C**, **D**, and **E**. Short Cu···Cu distances (2.7426(11)−2.8093(13) Å) were observed, such as in **C** (2.7634(13)−2.8386(10) Å) and in **D** (2.7322(10)−2.8653(12) Å). In addition, the Sn−Cu distances (3.0260(10)−3.1239(11) Å) are distinctly smaller than the sum of the van der Waals radii (3.60 Å).[28]

■ CONCLUSION

In conclusion, we have demonstrated that the concept of direct covalent attachment of Fc units to a T/E core (T = Ge, Sn; E = S) can be transferred to E = Se and Te. By treatment of $FcSnCl_3$ with K_2Se and K_2Te, two polynuclear complexes, **1** and **2** were obtained, which possess, however, different Sn/E structures. Further reaction of **1** with $Na_2S \cdot 9H_2O$ and $[Cu(PPh_3)_3Cl]$ led to the formation of a ternary Cu/Sn/E

dx.doi.org/10.1021/ic502026g | Inorg. Chem. 2014, 53, 12512−12518

(**3**; E = S and Se) complex containing two Fc units. The optical absorption properties and the electrochemical properties of **1**, **2**, and the previously synthesized sulfide complex **B** were examined by using UV−visible spectroscopy, CV, and DPV and compared. The UV−visible spectra of the three compounds are red-shifted as going from E = S through Se to Te, not only regarding the absorption bands of the Fc units, but also the bands resulting from p(E) → s,p(Sn) charge transfer despite the structural differences. In CV and DPV, all three compounds display slight electronic communication of adjacent Fc units, most notably in the case of **2** with shortest Fe···Fe distances. ^{119}Sn Mössbauer spectra reveal the different tin sites, while ^{57}Fe Mössbauer spectra point to almost similar electronic situation for all ferrocenyl entities, excluding a direct influence of the Sn_4Se_6 or Sn_3Te_2 cores on the metal atom within the ligand.

■ ASSOCIATED CONTENT

Ⓢ Supporting Information

Details on syntheses, ESI mass spectrometry, ^{119}Sn, ^{1}H, and ^{13}C NMR, UV−visible spectroscopy, electrochemical measurements, EDX spectroscopy, IR and Raman spectroscopy, X-ray diffraction, structure analyses, and Mössbauer spectroscopy. Crystallographic data in CIF format. This material is available free of charge via the Internet at http://pubs.acs.org.

■ AUTHOR INFORMATION

Corresponding Author

*E-mail: dehnen@chemie.uni-marburg.de. Fax: +49 6421 2825653. Phone: +49 6421 2825751.

Author Contributions

The manuscript was written through contributions of all authors. All authors have given approval to the final version of the manuscript. All authors contributed equally.

Notes

The authors declare no competing financial interest.

■ ACKNOWLEDGMENTS

This work was supported by the Deutsche Forschungsgemeinschaft (DFG) within the framework of SFB 1083. We are deeply indebted to Dr. M. Hołyńska for valuable help with the X-ray structure analyses, and we also thank A. Geese for his help in the preparation of compound **3**.

■ REFERENCES

(1) (a) Krebs, B. *Angew. Chem., Int. Ed.* **1983**, *22*, 113−134. (b) Dabbousi, B. O.; Bawendi, M. G.; Onitsuka, O.; Rubner, M. F. *Appl. Phys. Lett.* **1995**, *66*, 1316−1318. (c) Murray, C. B.; Kagan, C. R.; Bawendi, M. G. *Science* **1995**, *270*, 1335−1338. (d) Sheldrick, W. S.; Wachhold, M. *Angew. Chem., Int. Ed.* **1997**, *36*, 207−224. (e) Sheldrick, W. S.; Wachhold, M. *Coord. Chem. Rev.* **1998**, *176*, 211−322.

(2) (a) Zheng, N. *Science* **2003**, *299*, 1015−1015. (b) Zheng, N. F.; Bu, X. H.; Feng, P. Y. *Nature* **2003**, *426*, 428−432. (c) Feng, P. Y.; Bu, X. H.; Zheng, N. F. *Acc. Chem. Res.* **2005**, *38*, 293−303.

(3) (a) Soloviev, V. N.; Eichhöfer, A.; Fenske, D.; Banin, U. *J. Am. Chem. Soc.* **2000**, *122*, 2673−2674. (b) Soloviev, N. V.; Eichhöfer, A.; Fenske, D.; Banin, U. *J. Am. Chem. Soc.* **2001**, *123*, 2354−2364. (c) Zheng, N. F.; Bu, X. H.; Lu, H. W.; Zhang, Q. C.; Feng, P. Y. *J. Am. Chem. Soc.* **2005**, *127*, 11963−11965.

(4) (a) Dehnen, S.; Brandmayer, M. K. *J. Am. Chem. Soc.* **2003**, *125*, 6618−6619. (b) Brandmayer, M. K.; Clérac, R.; Weigend, F.; Dehnen, S. *Chem.—Eur. J.* **2004**, *10*, 5147−5157. (c) Zimmermann, C.; Anson, C. E.; Weigend, F.; Clérac, R.; Dehnen, S. *Inorg. Chem.* **2005**, *44*, 5686−5695. (d) Ruzin, E.; Fuchs, A.; Dehnen, S. *Chem. Commun.* **2006**, *46*, 4796−4798. (e) Dehnen, S.; Melullis, M. *Coord. Chem. Rev.* **2007**, *251*, 1259−1280. (f) Lips, F.; Dehnen, S. *Inorg. Chem.* **2008**, *47*, 5561−5563. (g) Ruzin, E.; Zent, E.; Matern, E.; Massa, W.; Dehnen, S. *Chem.—Eur. J.* **2009**, *15*, 5230−5244.

(5) (a) Fard, Z. H.; Clérac, R.; Dehnen, S. *Chem.—Eur. J.* **2010**, *16*, 2050−2053. (b) Fard, Z. H.; Hołyńska, M.; Dehnen, S. *Inorg. Chem.* **2010**, *49*, 5748−5752.

(6) (a) Fard, Z. H.; Xiong, L.; Müller, C.; Hołyńska, M.; Dehnen, S. *Chem.—Eur. J.* **2009**, *15*, 6595−6604. (b) Fard, Z. H.; Müller, C.; Harmening, T.; Pöttgen, R.; Dehnen, S. *Angew. Chem., Int. Ed.* **2009**, *48*, 4441−4444. (c) Heimann, S.; Hołyńska, M.; Dehnen, S. *Chem. Commun.* **2011**, *47*, 1881−1883. (d) Eussner, J. P.; Barth, B. E. K.; Leusmann, E.; You, Z.; Rinn, N.; Dehnen, S. *Chem.—Eur. J.* **2013**, *19*, 13792−13802.

(7) (a) Halvagar, M. R.; Fard, Z. H.; Dehnen, S. *Chem. Commun.* **2010**, *46*, 4716−4718. (b) Fard, Z. H.; Halvagar, M. R.; Dehnen, S. *J. Am. Chem. Soc.* **2010**, *132*, 2848−2849. (c) Halvagar, M. R.; Fard, Z. H.; Dehnen, S. *Chem.—Eur. J.* **2011**, *17*, 4371−4374.

(8) (a) Hauser, R.; Merzweiler, K. *Z. Anorg. Allg. Chem.* **2002**, *628*, 905−906. (b) Dörfelt, C.; Janeck, A.; Kobelt, D.; Paulus, E. F.; Scherer, H. *J. Organomet. Chem.* **1968**, *14*, 22−24.

(9) You, Z.; Dehnen, S. *Inorg. Chem.* **2013**, *52*, 12332−12334.

(10) You, Z.; Fenske, D.; Dehnen, S. *Dalton. Trans.* **2013**, *42*, 8179−8182.

(11) Ferguson, G.; Glidewell, C.; Opromolla, G.; Zakaria, C. M.; Zanello, P. *J. Organomet. Chem.* **1996**, *517*, 183−190.

(12) Lebold, T. P.; Stringle, D. L. B.; Workentin, M. S.; Corrigan, J. F. *Chem. Commun.* **2003**, *12*, 1398−1399.

(13) Pöhlker, C.; Schellenberg, I.; Pöttgen, R.; Dehnen, S. *Chem. Commun.* **2010**, *46*, 2605−2607.

(14) Ruzin, E. Ph.D. thesis, Philipps-Universität Marburg, 2007.

(15) Lippard, S. J.; Ucko, D. *Inorg. Chem.* **1968**, *7*, 1051−1056.

(16) Brand, R. A. *Normos Mössbauer fitting Program;* Universität Duisburg: Duisburg, Germany, 2007.

(17) Burla, M. C.; Caliandro, R.; Camalli, M.; Carrozzini, B.; Cascarano, G. L.; De Caro, L.; Giacovazzo, C.; Polidori, G.; Spagna, R. *J. Appl. Crystallogr.* **2005**, *38*, 381−388.

(18) Sheldrick, G. M. *SHELXL2013;* University of Göttingen: Germany, 2013.

(19) Mathiasch, B. *Z. Anorg. Allg. Chem.* **1977**, *432*, 269−274.

(20) Nayek, H. P.; Hilt, G.; Dehnen, S. *Eur. J. Inorg. Chem.* **2009**, *28*, 4205−4208.

(21) (a) Mathiasch, B. *Synth. React. Inorg. Met.-Org. Chem.* **1977**, *7*, 227−233. (b) Dräger, M.; Mathiasch, B. *Z. Anorg. Allg. Chem.* **1980**, *470*, 45−48. (c) Blecher, A.; Mathiasch, B.; Mitchell, T. N. *J. Organomet. Chem.* **1980**, *184*, 175−180. (d) Puff, H.; Breuer, B.; Schuh, W.; Sievers, R.; Zimmer, R. *J. Organomet. Chem.* **1987**, *332*, 279−288.

(22) Mathiasch, B. *J. Organomet. Chem.* **1976**, *122*, 345−350.

(23) Bratsch, S. G. *J. Phys. Chem. Ref. Data* **1989**, *18*, 1−21.

(24) Davies, A. G. Organotin Halides. In *Organotin Chemistry,* 2nd ed.; Wiley-VCH: New York, 2004; pp 166−167.

(25) Labande, A.; Ruiz, J.; Astruc, D. *J. Am. Chem. Soc.* **2002**, *124*, 1782−1789.

(26) MacDonald, D. G.; Eichhöfer, A.; Campana, C. F.; Corrigan, J. F. *Chem.—Eur. J.* **2011**, *17*, 5890−5902.

(27) (a) Kapusta, S.; Viehbeck, A.; Wilhelm, S. M.; Hackerman, N. *J. Electroanal. Chem.* **1983**, *153*, 157−174. (b) Herrero, E.; Climent, V.; Feliu, J. M. *Electrochem. Commun.* **2000**, *2*, 636−640. (c) Mohtadi, R.; Lee, W. K.; Van Zee, J. W. *Appl. Catal., B* **2005**, *56*, 37−42.

(28) Bondi, A. *J. Phys. Chem.* **1964**, *68*, 441−451.